Effects of Target Temperature on Ablation Volume During Temperature-controlled RFA of Breast Tumor

Sundeep Singh and Ramjee Repaka*
Indian Institute of Technology Ropar
* Room no. 219, Department of Mechanical Engineering, Indian Institute of Technology Ropar, Nangal Road, Rupnagar, Punjab-140001, India, ramjee.repaka@iitrpr.ac.in , ramjee.repaka@gmail.com

Abstract: Radiofrequency ablation (RFA) is the most promising, extensively studied and widely applied technique in clinical practice for the local treatment of solid tumors, viz., liver, kidney, lung, bone, brain and prostate. However, the application of RFA in the treatment of breast cancer is still in its developing stage. In this scenario, the present study aims at analyzing the efficacy of temperature-controlled RFA in breast tumor subjected to different target temperatures. A three-dimensional heterogeneous model of breast has been modeled with a spherical tumor of 1.5 cm. A closed-loop feedback PID controller has been incorporated in the numerical model to perform temperature-controlled RFA. The numerical simulation based on finite element method (FEM) reveals a strong dependence of ablation volume on the set target temperature during RFA. The findings of the numerical study may provide useful insights to clinical practitioners to perform RFA in a more reliable and effective way.

Keywords: Radiofrequency ablation, Breast cancer, Pennes bioheat equation, PID controller, Finite element method.

1. Introduction

Globally, breast cancer remains the second most leading cause of mortality among women. In 2012, an estimated 16.7 lakh cases of breast cancer were diagnosed worldwide with a mortality rate of 5.22 lakh [1]. In the Indian context, approximately one woman is dying out of every 2 women newly diagnosed with breast cancer [1]. The surgical management of breast cancer has evolved significantly from radical mastectomy to breast-conserving surgery. Although, breast conserving surgery remains the effective treatment modality for breast cancer treatment but still it is a highly invasive procedure with poor cosmetic results [2]. Thus, scientists have explored the feasibility and efficacy of non-surgical minimally invasive thermal ablation techniques with the intention of achieving equivalent efficacy with improved cosmesis [3, 4]. The minimal ablative thermal techniques also results in low cost, low morbidity and mortality rates, shorter recovery time and improved quality of life of the cancer patients [4].

Out of all the available thermal ablative techniques, RFA has received considerable attention because it is a faster technique exhibiting relatively fewer complications and low treatment cost as compared to the other treatment modalities. During RFA, electrode is inserted percutaneously into the target tissue with the aid of image guidance techniques, viz., computed tomography (CT), ultrasound (US), or magnetic resonance imaging (MRI), to destroy the tumor [5]. Once positioned, high-frequency alternate current (450-550 kHz) is delivered by the RF power generator that flows from the electrode to the ground pads placed at patient's back or thigh, forming a closed electric circuit. As the current flows through the human body, frictional (resistive or joule) heat is induced due to the agitation of free ions (Na^+, K^+, Cl^- etc.) present in the body to follow the polarity of high-frequency alternate current. This frictional heating, induced as a result of ionic agitation surrounding the electrode, leads to the destruction of tumor cells by the induction of protein coagulation within a few minutes above 50 ^oC and within seconds above 60 ^oC [6].

The mathematical models play a vital role in predicting the ablation volume and temperature distribution within the target tissue before the onset of RFA. Further, a significant number of numerical studies on mathematical modeling of RFA can be found in literature on hepatic cancer. On contrary, very limited computational studies are available on RFA of breast cancer [7-11] due to complexity associated in modeling heterogeneous breast models. In view of the above, the present numerical study focuses on

analyzing the effect of target tip temperature on the ablation volume produced during temperature-controlled RFA of breast tumor. A three-dimensional heterogeneous multi-layer model of breast has been developed in which spherical tumor of 1.5 cm has been embedded to mimic *in situ* tumor of early stages. A closed-loop feedback PID controller has been used to perform programmable temperature-controlled RFA of breast tumor. The induced thermal damage and temperature distribution within the target tissue is predicted by integrating the electric field distribution, Pennes bioheat equation and first-order Arrhenius rate equations in the mathematical model. The effect of temperature dependent changes in electrical and thermal conductivities of heterogeneous multi-layer breast model has been taken into account to achieve better correlation with the clinical RFA. Further, a non-linear piecewise model of blood perfusion has been used in the present study.

2. Mathematical Modeling

In the lower frequency range of 450–550 kHz, as is being used in RFA application, a quasi-static approximation can be used to solve the electro-magnetic problem without much loss of accuracy. This is because, the wavelength of the electromagnetic field is several orders of magnitude larger than the size of the active electrode for the frequency range considered during RFA. Hence, in the present study electric field distribution within the tissue has been computed by using the generalized Laplace equation

$$\nabla \cdot (\sigma \nabla V) = 0 \tag{1}$$

where σ is the electrical conductivity (S/m) and V is the electric potential (V).

The electric field intensity E (V/m) and the current density J (A/m^2) generated within the tissue can be computed from

$$\begin{aligned} \mathrm{E} &= -\nabla V \\ \mathrm{J} &= \sigma \mathrm{E} \end{aligned} \tag{2}$$

The volumetric heat generation rate Q_p (W/m^3) due to radiofrequency heating is defined as the product of current density (J) and electric field intensity (E), and is given by

$$Q_p = \mathrm{J.E} = \sigma . \mathrm{E}^2 \tag{3}$$

The temperature distribution within the heterogeneous multi-layer breast model has been evaluated by using well known Pennes bioheat equation [12]

$$\rho c \frac{\partial T}{\partial t} = \nabla \cdot (k \nabla T) - \rho_b c_b \omega_b (T - T_b) + Q_m + Q_p \tag{4}$$

where ρ is the density (kg/m^3), c is the specific heat capacity (J/kg.K), k is the thermal conductivity (W/m.K), ρ_b is the density of blood (1050 kg/m^3), c_b is the specific heat capacity of blood (3617 J/kg.K), ω_b is the blood perfusion rate (1/s), Q_p is the volumetric heating due to radiofrequency source (W/m^3), Q_m is the heat generated due to metabolic activity (W/m^3), T_b is the core blood temperature (assumed to be 37 ^{o}C) and T is the unknown tissue temperature to be computed.

The present study considers temperature dependence of electrical and thermal conductivities for both healthy tissue as well as tumor. The electrical and thermal conductivities of numerical model for the temperature range of 37 ^{o}C to 100 ^{o}C can be approximated by Eqs. (5) and (6), respectively [13].

$$\sigma(T) = \sigma_o \left[1 + 0.02 (T - T_b)\right] \tag{5}$$

$$k(T) = k_o + 0.0013 (T - T_b) \tag{6}$$

where σ_o and k_o are the constant electrical conductivity and thermal conductivity, respectively, at core body temperature, T_b = 37 ^{o}C represented in Table 1.

Earlier computational studies [14-15] have reported that, choice of microvascular perfusion algorithm has significant effects on final ablation zone dimensions during RFA. Therefore, the present study considers a non-linear model of blood perfusion, in which blood perfusion initially increases due to vasodilation of capillaries caused by heating of perfused tissue [16], and later decreases with time/induced damage, as represented in Eq. (7). Also, it is worth to mention that blood perfusion in breast tumor is more than the blood perfusion in the

surrounding healthy tissue, and the present study considers tumor perfusion as 5.3×10^{-3} s^{-1} [11].

$$\omega_b(t) = \begin{cases} \omega_{b,0} & \text{for } \Omega(t) \le 0 \\ \omega_{b,0}\left[1 + 25\Omega(t) - 260\Omega(t)^2\right] & \text{for } 0 < \Omega(t) \le 0.1 \\ \omega_{b,0}\exp\left[-\Omega(t)\right] & \text{for } \Omega(t) > 0.1 \end{cases} \quad (7)$$

where $\omega_{b,0}$ is the constant blood perfusion of the tissue and has been provided in Table 1, and $\Omega(t)$ is the induced thermal damage.

The induced damage (or damage integral) has been computed using the well-established first order Arrhenius equation [17].

$$\Omega(t) = \int_0^t A e^{\frac{-E_a}{RT(t)}} dt \quad (8)$$

where t is the treatment time, A is a frequency factor (s^{-1}), E_a is the activation energy barrier (J/mol) and R is the universal gas constant (8.314 J/mol K). In the present study, A and E_a for the bulk tissue domain have been considered as 1.18×10^{44} s^{-1} and 3.02×10^{5} J/mol, respectively [18]. In the context of tissue damage, a damage integral of $\Omega(t)=1$ corresponds to 63% probability of cell death and damage integral of $\Omega(t)=4.6$ corresponds to 99% probability of cell death at a specific point. In the present study, the damage integral value of $\Omega(t) = 1$ has been employed as a critical threshold to represent the tissue death [11, 18].

The temperature-controlled RFA is the reliable and commonly used technique in clinical practices. This is because the temperature-controlled RFA eradicates any adverse effects of charring and overheating of the biological tissue such as, drastic decline in electrical and thermal conductivities and poor image resolution. During temperature-controlled mode, initially, the applied voltage increases monotonically till the target temperature is reached and declines afterward to limit the set target temperature, but still it may rise if target temperature falls. In the present study, programmable temperature-controlled mode has been modeled by incorporating proportional-integral-derivative (PID) controller to limit the target temperature to a set point during RFA, as shown in Fig. 1. The PID controller is a closed-loop feedback system that gauges the input error, i.e., the difference between set tip temperature and current tip temperature, and accordingly modulates the required input voltage for dynamic system [19, 20]. The input voltage V (t), applied on the active part of the electrode is given by

$$V(t) = K_p e(t) + K_i \int_0^t e(\tau)d\tau + K_d \frac{d}{dt}e(t) \quad (9)$$

where V is the applied voltage (V), e is the error that is continuously fed back to the PID controller, and K_p (0.02), K_i (0.01) and K_d (0.001) are the proportional, integral and derivative gains, respectively [19].

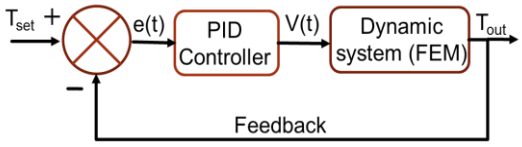

Figure 1. PID closed loop control system with continuous feedback.

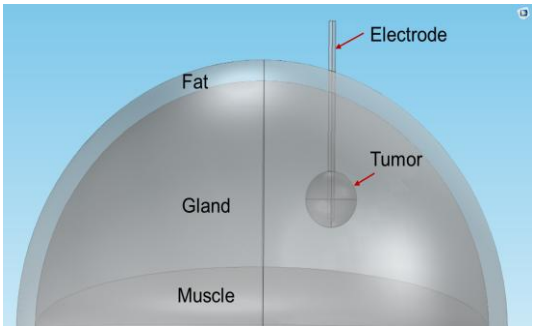

Figure 2. Schematic of three-dimensional two-compartment heterogeneous multi-layer breast model with mono-polar electrode in COMSOL®.

Figure 2 shows the three-dimensional multi-layer model of breast comprising of fat, glandular and muscular tissues [21]. A 1.5 cm diameter spherical tumor has been embedded into the upper outer portion of the glandular tissue to replicate clinical scenario. A mono-polar electrode with an active part of 1.4 cm has been inserted into the tumor. The temperature at the electrode tip is monitored and the power is adjusted accordingly to maintain the tip temperature below the pre-set target temperature with the help of PID controller. Further, eight different values of target temperature, viz., 60

°C, 65 °C, 70 °C, 75 °C, 80 °C, 85 °C, 90 °C and 95 °C have been considered to determine the effect of target temperature on ablation volume during RFA. Here, the maximum tip temperature value has been judiciously considered to be below 100 °C to mitigate any chances of charring and tissue carbonisation close to the active part of the electrode. The material properties used in present study have been tabulated in Table 1 [9, 11, 18, 21].

Table 1: Electrical and thermo-physical properties of different materials used in RFA modelling at 460 kHz [9, 11, 18, 21].

Material	σ	c	k	ρ	Q_m ($\times 10^3$)	ω_b ($\times 10^{-3}$)
Gland	0.563	2960	0.33	1041	0.7	0.5
Fat	0.0254	2348	0.21	911	0.4	0.2
Muscle	0.439	3421	0.49	1090	0.7	0.8
Tumor	0.71	3770	0.48	1050	13.6	5.3
Electrode	10^8	840	18	6450	–	–
Trocar	10^{-5}	1045	0.026	70	–	–

3. Numerical Simulations

The three-dimensional model of heterogeneous breast along with the spherical tumor and monopolar electrode have been constructed using geometry interface of COMSOL®. The initial voltage of the entire breast domain before the onset of RFA has been considered to be zero. The electrode potential at the active part of electrode has been set to variable voltage source $V(t)$ computed by PID controller. A zero electric potential has been applied at the bottom surface of the breast model to simulate a ground pad. An electrical insulation boundary condition has been applied for the insulated part of the electrode. The initial temperature of entire breast model has been considered to be same as that of the core human body temperature, i.e., at 37 °C. The initial temperature of electrode has been considered to be 25 °C simulating the ambient room conditions. The outer surface of the breast and electrode (outside the tissue domain) have been assumed to be subjected to natural convection (h_{conv} =13.5 W/m^2.K and T_∞ =25 °C). Further, the present study utilizes the electric currents (ec) physics of AC/DC module, bioheat transfer (ht) physics of Heat Transfer module, Global ODEs and DAEs (ge) and Domain ODEs and DAEs (dode) of COMSOL Multiphysics to solve the coupled thermo-electric problem. A programmable temperature-controlled RFA has been performed by employing a PID controller to monitor and maintain the tip temperature of RF electrode below a set target temperature. In the present study, treatment time has been assumed to be 20 minutes for all simulations.

The meshing of the computational domain has been done using heterogeneous tetrahedral mesh elements, with a finer mesh size close to the electrode surface. All the mesh elements have been generated using in built free mesh generator of COMSOL after conducting grid independence test. The relative tolerance for the electric field interface and heat transfer interface has been set to be 0.0001. All simulations have been carried out on a Dell Precision Tower7810 workstation with eight Core 3.1 GHz Xeon processor and 64 GB RAM.

4. Results and discussion

In the present study, the effect of target temperature on input voltage requirement, temperature distribution and ablation volume during temperature-controlled RFA of breast tumor has been analyzed. The variation of input voltage with time for different values of tip temperature has been shown in Fig. 3. It can be clearly seen from Fig. 3 that, the input voltage requirement increases as the tip temperature increases. Further, it has been found that the maximum voltage value increases from 11.62 V to 20.15 V, as the tip temperature shifts from 60 °C to 95 °C during temperature-controlled RFA of breast tumor. Moreover, negligible variation prevails among the time required to attain the pre-set target temperature (i.e., the time at which maximum voltage occurs) for all cases, as has been depicted in Fig. 3.

A comparison of damage volume produced (corresponding to Ω =1) after 20 minutes of temperature-controlled RFA for different values of target temperature has been presented in Fig. 4. It is evident from Fig. 4 that, the maximum

ablation volume is produced when the target temperature is 95 ^{o}C during RFA. It is worth to mention that zero ablation volume has been produced for the case of 60 ^{o}C target temperature during RFA of breast tumor.

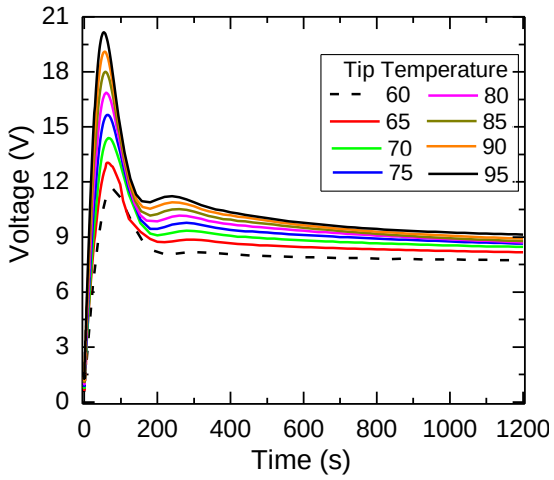

Figure 3. Variation of input voltage with time for different tip temperatures.

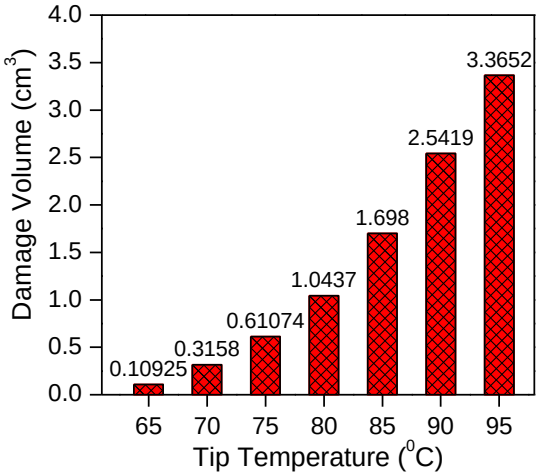

Figure 4. Variation of damage volume with tip temperature during temperature-controlled RFA.

Figure 5 depicts the temperature distribution with distance from the electrode (perpendicular to the electrode surface that passes through the center of the tumor) for different values of target temperature after 20 minutes of temperature-controlled RFA. It can be clearly seen from Fig. 5 that, there is a significant variation of temperature at the tumor periphery for different values of target temperatures. It can be observed from Fig. 5 that, the temperature attained at the tumor periphery is below 50 ^{o}C for the target temperatures up to 70 ^{o}C after 20 minutes of temperature-controlled RFA. Hence, the target temperature below 70 ^{o}C is insufficient for attaining complete tumor necrosis of 1.5 cm diameter breast tumor after 20 minutes of RFA application. Furthermore, the temperature at the tumor periphery is greater than 60 ^{o}C for the target temperature of 90 and 95 ^{o}C, which ascertains complete necrosis of breast tumor during RFA. Moreover, it can be observed that the maximum temperature has been achieved close to the active part of electrode surface, and temperature declines as the distance from the electrode increases for all cases.

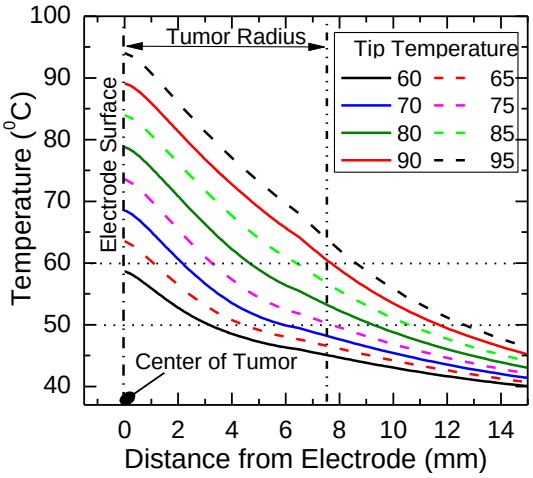

Figure 5. Temperature distribution for different tip temperatures during RFA as a function of distance from the electrode (measured perpendicular to the electrode surface that passes through the center of tumor).

The variation of damage field distributions corresponding to different values of target temperatures considered in the present study have been depicted in Fig. 6. It can be clearly seen from Fig. 6 that, significant variation in the damage field distribution prevails for different target temperature values during RFA. Further, it is evident form Fig. 6 that, complete necrosis of breast tumor has only been attained when the target temperature is greater than 90 ^{o}C during temperature-controlled RFA. Thus, the present study demonstrates the significance of pre-clinical modelling to highlight the effect of target

temperature on the ablation volume attained during RFA application of breast tumor.

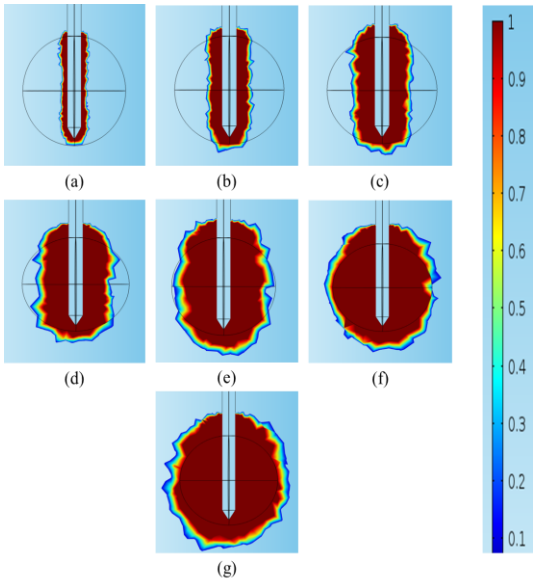

Figure 6. Damage field distributions for different target temperatures: (a) 65 ^{o}C; (b) 70 ^{o}C; (c) 75 ^{o}C; (d) 80 ^{o}C; (e) 85 ^{o}C; (f) 90 ^{o}C and (g) 95 ^{o}C.

5. Conclusion

A three-dimensional multi-layer breast model has been developed to simulate the clinical RFA of breast cancer. A thermo-electric analysis has been performed by utilizing a closed-loop feedback PID controller to perform temperature-controlled RFA of two-compartment breast model with mono-polar electrode. An attempt has been made in this study to find the relation between the target temperature and the ablation volume produced during temperature-controlled RFA of breast tumor. The study revealed that, the complete necrosis of 1.5 cm tumor diameter occurred only for the cases where the set target temperature is greater than 90 ^{o}C for 20 minutes of RFA. Further, it has been found that, the set target temperature of 70 ^{o}C and below is insufficient to raise the tumor periphery temperature above 50 ^{o}C even after 20 minutes of RFA procedure. Also, the effect of target temperature on the input voltage requirement has been studied. The findings presented in the study may provide useful insights to clinical practitioners to perform RFA of breast tumor in a more reliable and effective way.

6. Acknowledgments

Authors would like to acknowledge Science and Engineering Research Board, Department of Science and Technology, Government of India, for providing the grant (SB/FTP/ETA-0135/2013) to pursue the present research work. Authors would also like to acknowledge Indian Institute of Technology Ropar for providing essential infrastructure to carry out the present research.

7. References

1. J. Ferlay, I. Soerjomataram, R. Dikshit, et al., GLOBOCAN 2012 v1.0, Cancer Incidence and Mortality Worldwide: International Agency for Research on Cancer, <http://globocan.iarc.fr>.
2. A.K. Bajaj, P.S. Kon, K.C. Oberg, D.A. Miles, Aesthetic outcomes in patients undergoing breast conservation therapy for the treatment of localized breast cancer, *Plast. Reconstr. Surg.*, **114(6)**, pp. 1442–1449 (2004).
3. K.F. Chu and D.E. Dupuy, Thermal ablation of tumours: biological mechanisms and advances in therapy, *Nature Reviews Cancer*, **14(3)**, pp. 199-208 (2014).
4. T. Nguyen, E. Hattery, V.P. Khatri, Radiofrequency ablation and breast cancer: a review, *Gland Surgery*, **3(5)**, pp. 128–135 (2014).
5. G.S. Gazelle, S.N. Goldberg, L. Solbiati, T. Livraghi, Tumor ablation with radio-frequency energy 1, *Radiology*, **217(3)**, pp. 633-646 (2000).
6. M.W. Miller, M.C. Ziskin, Biological consequences of hyperthermia, *Ultrasound Med. Biol.*, 15 (8), pp. 707-722 (1989).
7. V. Ekstrand, H. Wiksell, L. Schultz, *et al.*, Influence of electrical and thermal properties on RF ablation of breast cancer: is the tumour preferentially heated?, *Biomed. Eng. Online*, **4(1)**, (2005).
8. V. Quaranta, G. Manenti, F. Bolacchi, *et al.*, FEM analysis of RF breast ablation: multiprobe versus cool-tip electrode, *Anticancer Research*, **27(2)**, pp. 775-784 (2007).
9. Z. Wang, I. Aarya, M. Gueorguieva, *et al.*, Image-based 3D modeling and validation of radiofrequency interstitial tumor ablation using a tissue-mimicking breast phantom, *International Journal of Computer Assisted Radiology and Surgery*, **7(6)**, pp. 941–948 (2012).

10. S. Singh, A. Bhowmik, R. Repaka, Radiofrequency ablation of malignant breast tumor: A numerical study, *Proc. 23rd National Heat and Mass Transfer Conference and 1st International ISHMT-ASTFE Heat and Mass Transfer Conference*, 17-20 December 2015, Thiruvananthapuram, India.
11. S. Singh, A. Bhowmik, R. Repaka, Thermal analysis of induced damage to the healthy cell during RFA of breast tumor, *Journal of Thermal Biology*, **58**, pp. 80–90 (2016).
12. H.H. Pennes, Analysis of tissue and arterial blood temperatures in the resting human forearm, *J. Appl. Physiol*., **85(1)**, pp. 5-34 (1998).
13. B. Zhang, M.A. Moser, E.M. Zhang, *et al.*, Study of the relationship between the target tissue necrosis volume and the target tissue size in liver tumours using two-compartment finite element RFA modelling, *International Journal of Hyperthermia*, **30(8)**, pp. 593-602 (2014).
14. D.J. Schutt and D. Haemmerich, Effects of variation in perfusion rates and of perfusion models in computational models of radio frequency tumor ablation, *Medical Physics*, ***35*(8)**, 3462–3470 (2008).
15. S. Singh, R. Repaka, Pre-clinical modelling and simulation of hepatic radiofrequency ablation, *Proc COMSOL Conference 2015*, 29-30 October 2015, Pune, India.
16. J.P. Abraham and E. M. Sparrow, A thermal-ablation bioheat model including liquid-to-vapor phase change, pressure-and necrosis-dependent perfusion, and moisture-dependent properties, *Int. J. Heat Mass Transfer.*, **50(13)**, pp. 2537-2544 (2007).
17. F.C. Henriques, Studies of thermal injury V: The predictability and significance of thermally induced rate processes leading to irreversible epidermal injury, *Arch. Pathol*, **43**, pp. 489-502 (1947).
18. S. Singh, R. Repaka, Temperature-controlled radiofrequency ablation of different tissues using two-compartment models, *International Journal of Hyperthermia*, online version available at <http://dx.doi.org/10.1080/02656736.2016.1223890> (2016).
19. D. Haemmerich, J.G. Webster, Automatic control of finite element models for temperature-controlled radiofrequency ablation, *Biomedical engineering online*, **4(1)** (2005).
20. M. Jamil, E.Y.K. Ng, Quantification of the effect of electrical and thermal parameters on radiofrequency ablation for concentric tumour model of different sizes, *Journal of Thermal Biology*, **51**, pp. 23-32 (2015).
21. E.Y.K. Ng, N.M. Sudharsan, An improved three-dimensional direct numerical modelling and thermal analysis of a female breast with tumour, *J. Eng. Med*., **215(1)**, pp. 25-37 (2001).